Wood Science and Technology (2025) 59:78
https://doi.org/10.1007/s00226-025-01673-3

ORIGINAL

Organosilicon compound reactivity with biologically and chemically degraded Scots pine as determined by $^{1}H–^{13}C$ HSQC NMR

Daniel J. Yelle[1] · **Magdalena Broda**[2]

Received: 29 January 2025 / Accepted: 30 May 2025

Abstract

Ancient archeological wooden artifacts hold important stories from our history that can only be retold through wood conservation. Understanding the detailed mechanisms of how to stabilize these fragile artifacts dimensionally is necessary to effectively preserve them for the next generations. In this study, highly effective organosilicons are used to treat and infiltrate model degraded wood. We used wood dissolution techniques, in conjunction with two-dimensional nuclear magnetic resonance spectroscopy, to characterize the changes occurring to native wood cell wall polymers before and after organosilicon treatments. Methyltrimethoxysilane was shown to be the mildest organosilicon towards wood polymer depolymerization in the model woods, while the alkoxysilane with a mercaptopropyl group resulted in more dramatic cell wall depolymerization, removing lignin linkages and polysaccharides. The siloxane treatment did depolymerize the model woods as well, giving more intermediate cell wall depolymerization and leading to reduction of the α-carbonyl in G-2′ guaiacyl units in lignin. We hypothesize that the organosilicon treatments can effectively infiltrate cell wall matrices, partially depolymerize wood cell wall polymers, and meld the truncated wood polymers together to stabilize cell wall dimensions.

✉ Daniel J. Yelle
daniel.j.yelle@usda.gov

[1] Forest Products Laboratory, Forest Biopolymers Science and Engineering, USDA Forest Service, One Gifford Pinchot Drive, Madison, MI 53726, USA

[2] Department of Wood Science and Thermal Techniques Faculty of Forestry and Wood Technology , Poznan University of Life Sciences, Wojska Polskiego str. 38/42, 60-637 Poznan, Poland

Published online: 07 July 2025

Abbreviations

A1	Methyltrimethoxysilane
A2	(3-Mercaptopropyl)trimethoxysilane
ASE_v	Volumetric anti-shrink efficiency coefficient
CP	Contemporary pine wood (non-degraded)
ChP	Chemically degraded pine wood
BP	Biologically degraded pine wood
S1	1,3-Bis-[(diethylamino)-3-(propoxy) propan-2-ol]-1,1,3,3-tetramethyldisiloxane
S_v	Volumetric shrinkage

Introduction

Wood is a natural material, and as such, it is susceptible to decomposition by various biotic and abiotic factors, including fungi, bacteria, insects, mechanical forces of wind, precipitation, temperature fluctuations, air pollutants, and UV radiation (Blanchette et al. 1989; Reinprecht 2016; Marais et al. 2022). Degradation processes shorten the service life of commercial wood and limit its broader application for industrial purposes; they also affect historical wooden artifacts, irreversibly depriving them of aesthetics and historical value. Therefore, several treatments and methods have been developed for industrial and historical wood to slow deterioration and prolong its lifespan (Hill 2007; Gérardin 2016; Sandberg et al. 2017; Broda and Hill 2021; Spear et al. 2021; Zelinka et al. 2022).

Conservation of historical wood is even more challenging than the preservation of commercial wood since the object of interest is usually already degraded to some extent and requires not only protection against further degradation but also proper consolidation to retain structural integrity. A special case is the conservation of waterlogged archaeological wood, where adding an appropriate dimensional stabilization treatment during drying is necessary to counteract the capillary forces of water evaporating from water-saturated wood that may otherwise cause irreversible distortions, shrinkage, cracking, or even disintegration of a wooden artifact (Grattan 1987; Unger et al. 2001; Grattan et al. 2006). Since the existing methods for waterlogged wood conservation are not free of drawbacks (Glastrup et al. 2006; Hoffmann 2010; Mortensen et al. 2012; Morgós et al. 2015; Vorobyev et al. 2019; Afshar et al. 2020; Broda and Hill 2021), there is a need to search for new, more effective treatments. Therefore, we investigated the usefulness of various organosilicon compounds as consolidants for waterlogged wood (Smith 2002; Kavvouras et al. 2009; Broda et al. 2020, 2023; Zhou et al. 2024).

Extensive research on new conservation agents requires large amounts of wood material, preferably similar and homogeneously degraded, to ensure reliable and comparable results of experiments and analyses. Unfortunately, waterlogged archaeological objects are usually heterogeneously decayed, with outer layers typically more degraded than core zones, so it is hard to obtain a great number of similar wood samples from them (Hoffmann and Jones 1989; Björdal et al. 2000; Wu et al. 2022; Han et al. 2022, 2023). Moreover, such artifacts often have historical value

and cannot be used as research material. In such cases, the solution may be the use of a model wood material obtained in an artificial, controlled degradation process that mimics naturally decayed wood (Franceschi et al. 2008; Kennedy and Pennington 2014; Tahira et al. 2017; Liu et al. 2019; Albelda Berenguer et al. 2019; Wakefield et al. 2020).

In our previous studies, we prepared a model wood material applying two different degradation methods: biological decomposition using the brown rot fungus *Coniophora puteana* (Shum.: Fr.) P. Karst and chemical (alkaline) degradation with 50% NaOH solution (Broda et al. 2022a, b). Wood decay by brown rot fungi causes selective decomposition of polysaccharides with some changes in lignin structure (Pandey and Pitman 2003; Zhu et al. 2022; Belt et al. 2024). In turn, alkaline hydrolysis using NaOH solution effectively degrades lignin but additionally decomposes hemicelluloses. Higher NaOH concentrations can affect cellulose, leading to its decrystallization and recrystallization from native cellulose I to cellulose II (Nishiyama et al. 2000; Miura and Nakano 2015; Bakri et al. 2016; Xu et al. 2020).

We measured selected properties of model degraded wood (Broda et al. 2022a, b) and then used this wood for treatment with selected organosilicon compounds. We found that the stabilizing effectiveness of the applied chemicals varies depending on the type of wood conserved (Broda and Plaza 2023; Broda et al. 2024). To better understand the observed differences, we investigated the stabilizing mechanisms using synchrotron-based X-ray fluorescence microscopy (XFM) and nanoindentation (Broda et al. 2024) and analyzed alterations in the wood nanostructure (Broda et al. 2025) and the macromolecular structure of main wood polymers in biologically and chemically degraded model pine wood (Yelle and Broda 2025). To obtain a more comprehensive picture of the effect of organosilicon on wood differing in chemical composition and structure, though, more detailed knowledge about the reactivity of these chemicals with wood cell wall polymers is necessary.

This research investigated how changes in the chemical composition of artificially degraded wood affect wood reactivity with organosilicon compounds used for its impregnation regarding the dimensional wood stabilization obtained. Such knowledge can help explain the stabilizing mechanism of organosilicons on wood, which is necessary to develop new and effective treatments tailored to the needs of individual wooden artifacts. To achieve this, wood treated with three organosilicon compounds was used for the study. The organosilicons selected were two alkoxysilanes (Methyltrimethoxysilane and (3-Mercaptopropyl)trimethoxysilane) and 1,3-Bis-[(diethylamino)−3-(propoxy)propan-2-ol]−1,1,3,3-tetramethyldisiloxane, which have already proven effective in stabilizing waterlogged wood dimensions in our earlier studies (Broda et al. 2020; Broda and Yelle 2022). The stabilizing effect was measured through changes in wood dimensions before and after treatment concerning the dimensional changes of untreated wood. Wood chemistry was analyzed using two-dimensional (2D) $^{1}H–^{13}C$ heteronuclear single quantum coherence (HSQC) solution-state nuclear magnetic resonance (NMR) spectroscopy that allows the identification of structural changes in the main wood polymers – lignin, cellulose, and hemicelluloses, both qualitatively and semi-quantitatively (Maunu 2002; Holtman et al. 2004; Hedenström et al. 2009; Yelle et al. 2013, 2014; Lourenço et al. 2020; Koso et al. 2020; Fliri et al. 2023). This NMR method is also useful for investigating the

reactivity of wood polymers with various modification agents (Lu and Ralph 2003; Yelle et al. 2011a; Yelle and Ralph 2016; King et al. 2018; Namyslo et al. 2021) and has already been successfully employed in our previous research on waterlogged wood conservation using organosilicon compounds (Broda and Yelle 2022).

Materials and methods

Contemporary Scots pine (*Pinus sylvestris* L.) wood purchased from a commercial timber merchant (Poland) was used in this research. Wood was cut into small cuboid specimens (20 mm × 20 mm × 10 mm in the radial, tangential, and longitudinal directions, respectively) free from visible defects. A separate set of specimens were subjected to artificial degradation under laboratory conditions: biological decay using the brown rot fungus *Coniophora puteana* (Shum.: Fr.) P. Karst (specimens were placed on glass supports in Kole flasks on 5% malt agar pre-inoculated with the fungus and incubated at 24 ± 1 °C and 70 ± 5% relative humidity in a growing chamber for 8 weeks, then taken out and cleaned of the mycelium), and alkaline degradation using 50% NaOH (specimens were submerged in alkaline solution for 3 weeks at 24 ± 1 °C, then washed with distilled water until pH of 7 was obtained), as described previously (Broda et al. 2022a). Biologically (BP) and chemically (ChP) degraded specimens were kept in distilled water to mimic waterlogged wood. Before impregnation, water was exchanged into 96% ethanol to ensure proper penetration of organosilicons into the wood tissue and avoid their polymerization in the outer parts of specimens, while sound undegraded (CP) wood specimens were used in an air-dry state. Structural and physical properties of these wood types were measured using: an analytical balance with 0.01 mg readability (mass loss, %), the ratio of the sample weight to its volume after air-drying and conditioning (bulk density, g cm^{-3}), a nitrogen absorption method (total pore volume, cm^3 g^{-1}), and a method that utilizes deuterium exchange in a Dynamic Vapor Sorption (DVS) apparatus (free hydroxyls, mmol g^{-1}), and are thoroughly discussed in previous studies (Broda et al. 2022a, b).

All wood types were then treated with 50% ethanol solutions of selected organosilicon compounds (Fig. 1) using the oscillating vacuum-pressure method (−0.9 bar for 0.5 h and 10 bars for 6 h, repeated 6 times every 24 h to increase diffusion of organosilicon molecules into wood tissue; between the cycles wood specimens were left in the organosilicon solution) (Broda et al. 2020):

- Methyltrimethoxysilane, $CH_3Si(OCH_3)_3$ (**A1**),
- (3-Mercaptopropyl)trimethoxysilane, $HS(CH_2)_3Si(OCH_3)_3$ (**A2**),
- 1,3-Bis-[(diethylamino)−3-(propoxy)propan-2-ol]−1,1,3,3-tetramethyldisiloxane, $[(C_2H_5)_2NCH_2CH(OH)CH_2O(CH_2)_3Si(CH_3)_2]_2O$ (**S1**).

After impregnation, wood specimens were removed from organosilicon solutions and air-dried slowly at room temperature (21 ± 1 °C) and relative humidity of 45 ± 5% for four weeks. Additionally, untreated pine specimens of each type were used as a reference. Their dimensions were measured in all three anatomical directions

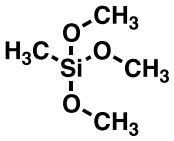

Methyltrimethoxysilane (**A1**)

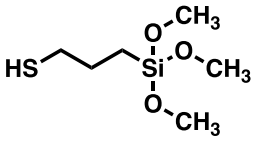

(3-Mercaptopropyl)trimethoxysilane (**A2**)

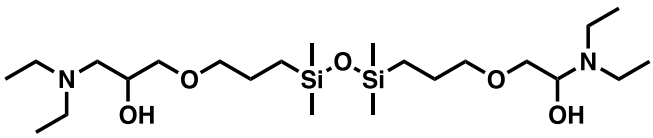

1,3-Bis-[(diethylamino)-3-(propoxy)propan-2-ol]-1,1,3,3-tetramethyldisiloxane (**S1**)

Fig. 1 Chemical structures of organosilicon compounds used for contemporary pine wood impregnation

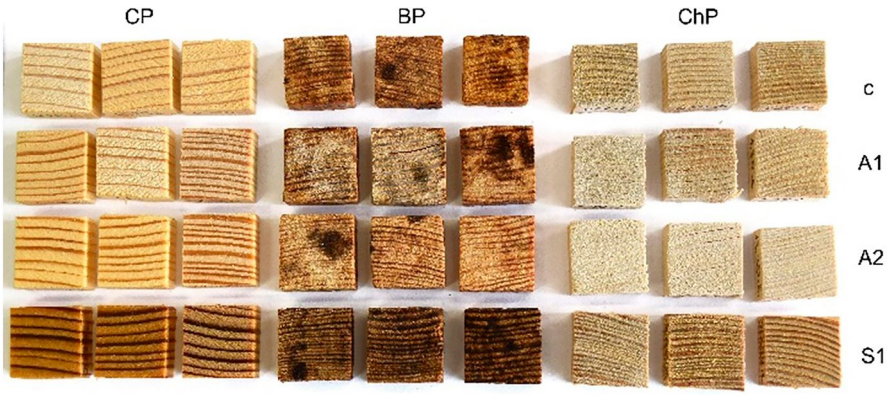

Fig. 2 A photo of the air-dried Scots pine specimens (post-impregnation) used in this study. The three model wood types are shown here as sound control pine (CP), biologically degraded pine (BP), and chemically degraded pine (ChP) wood, along with the four treatment types: untreated control c, A1, A2, and S1

with a digital caliper (± 0.01 mm) to calculate wood shrinkage and anti-shrink efficiency. Figure 2 shows the post-impregnated air-dried specimens used in this study.

Impregnation effectiveness and the stabilizing effect of individual organosilicon compounds were assessed based on the weight-percent gain (*WPG*), volumetric shrinkage (S_v), and anti-shrink efficiency coefficient (ASE_v) values calculated according to standard equations (below) from wood dimensions before and after treatment (Broda et al. 2020, 2024):

$$WPG = \frac{W_1 - W_0}{W_0} \times 100$$

where W_0 is the estimated dry mass of the specimen before treatment, and W_1 is the dry mass of the specimen treated with selected organosilicon compound,

$$S_v = \frac{V_0 - V_1}{V_0} \times 100$$

where V_0 is the initial volume of the specimen and V_1 is the final volume of the specimen after air-drying,

$$ASE_v = \frac{S_{vu} - S_{vt}}{S_{vu}} \times 100$$

where S_{vu} and S_{vt} are the volumetric shrinkage of the untreated and treated specimen, respectively.

To prepare wood samples for NMR analysis, three air-dried specimens were pooled from each of the three wood types (sound control, biologically degraded, chemically degraded) within the four treatment types (untreated, A1, A2, S1), thus making twelve total specimens. Each of the three specimens within a pooled sample was sliced with a knife in the radial direction into 1-mm-thick sections. The sliced and pooled samples were placed in separate 50 ml ZrO_2 jars. Then, three 20 mm ZrO_2 balls were added to each jar. Wood was milled using a Retsch PM-400 planetary ball mill (Newtown, PA) for 24 h in the following cycles: 300 rpm, 20 min milling, 10 min pause. Such conditions are necessary to keep the wood temperature below 50 °C, preventing its thermal degradation and altering the chemical composition. After this initial milling, the balls were removed and shaken in the copper sieve to recover all wooden particles covering their surfaces. Then, ten 10 mm ZrO_2 balls were added to each jar with a pre-milled sample, and the milling was continued under the same conditions as previously described. The milled wood recovery procedure was repeated, and the remaining milled wood was scraped from the jar and weighed (Broda and Yelle 2022). The principal caveat of the wood dissolution technique is that the samples must first be ball-milled, but research to date indicates that this procedure causes only minor increases in detectable cleaved lignin structures (Ikeda et al. 2002; Kim and Ralph 2010; Yang et al. 2021). Furthermore, we have drastically decreased the rpm of the planetary ball-mill from the typical 600 rpm for wood samples down to 300 rpm to lessen any structural effects seen from ball-milling alone.

Approximately 30 mg of each milled sample was dissolved with 500 µl DMSO-d_6 in an NMR tube with dimensions 17.8 cm in length and 5 mm in diameter. A separate set of CP samples (untreated CP, CP-A1, CP-A2, and CP-S1) were dissolved in 500 µl dimethylacetamide-d_9 in an NMR tube to assess if the NMR solvent (i.e., DMSO-d_6) could cause the demethylation of a silicon atom in siloxanes and foster the reduction of α-carbonyls on guaiacyl units. The tubes were sonicated at 35 °C for 1 h to accelerate wood dissolution (Hossain et al. 2021). Clear, homogenous wood solutions were used for NMR analysis. NMR spectra were acquired using a Bruker-Biospin (Rheinstetten, Germany) AVANCE III HDTM 500 MHz spectrometer fitted with a nitrogen-cooled 5 mm Prodigy™ TCI gradient cryoprobe with inverse geometry. The one-bond ^{1}H–^{13}C HSQC spectra were obtained using the adiabatic Bruker

pulse program hsqcetgpsisp2.2 and processed as previously described (Yelle et al. 2008a).

The advantages of adiabatic pulses are their compensation for all pulse imperfections. For example, off-resonance effects are eliminated. This is accomplished through several steps: (1) By replacing most crucial rectangular inversion pulses with adiabatic pulses, the offset dependence of ^{13}C-^{1}H HSQC spectra is removed and the active bandwidth is essentially unlimited. (2) Chemical shift refocusing is also achieved by applying the adiabatic pulse twice to correct phase errors introduced by the first pulse, which refocuses magnetization exactly. *J*-refocusing allows for making ^{13}C-^{1}H spin-spin couplings more uniformly distributed by matching the sweep rate of the adiabatic pulse with the natural distribution of the *J*-couplings. It is this point that makes adiabatic HSQC's able to be deemed quantitative. (3) Adiabatic heteronuclear decoupling covers an unlimited bandwidth. For example, the entire ^{13}C spectral range is decoupled with efficient side-band suppression. (4) Adiabatic pulses have a high tolerance to inhomogeneity of the RF field, thus eliminating the time-consuming calibrations of RF power required for conventional pulses (Kupče and Freeman 2007; de Graaf and Nicolay 1997).

To semi-quantitatively analyze the wood polymer structures present in the obtained spectra, specific chemical shifts of native structural units (such as the acetylated galactoglucomannan units and α- & β-reducing endgroups in hemicelluloses, as well as the guaiacyl units, β-aryl ether, and phenylcoumaran subunit linkages in lignin) were integrated using Bruker TopSpin 3.6.2 software and referenced to the lignin methoxyl group since it is known as the most stable functional group in wood polymers (Lundquist and Lundgren 1972). Performing such integrations on 2D NMR data from polymeric materials is sensitive to cross-peak overlap. Thus, all integrations were measured only on intense well-resolved cross-peaks; three separate integration calculations were obtained on each contour within the same sample (at 60, 80, and 120 contour levels) with the averages reported. Semi-quantification data can be found in the supplementary information along with the lignin subunit linkages (β-O-4 and β−5) on the basis of 100 guaiacyl units (Table S.I. 1).

Results

To better understand how the undegraded (CP) and model degraded (BP and ChP) pine wood interacted with the organosilicon compounds, the HSQC NMR spectra were analyzed. A key to the macromolecular structures found in each spectrum is shown in Fig. 3. The wood cell wall polymers we focused on in this study included: the major lignin substructures β-aryl ethers, phenylcoumarans, pinoresinols, cinnamyl alcohol endgroups, and the lignin methoxyls; G-2, G-2′, G-5/6, and G-6′. The G-2′ and G-6′ represent the α-carbonyl version of guaiacyl units; the C-2 and C-3 *O*-acetylated mannan (2-*O*-Ac-β-D-Man*p*, and 3-*O*-Ac-β-D-Man*p*) as well as the diacetylated mannan (2,3-*O*-Ac-β-D-Man*p*); polysaccharide anomerics which include D-glucan, D-xylan, D-mannan, D-galactan, and L-arabinan as the major sugars; and other anomerics such as 4-*O*-methyl-α-D-glucuronic acid units and the reducing endgroups of the main polysaccharides.

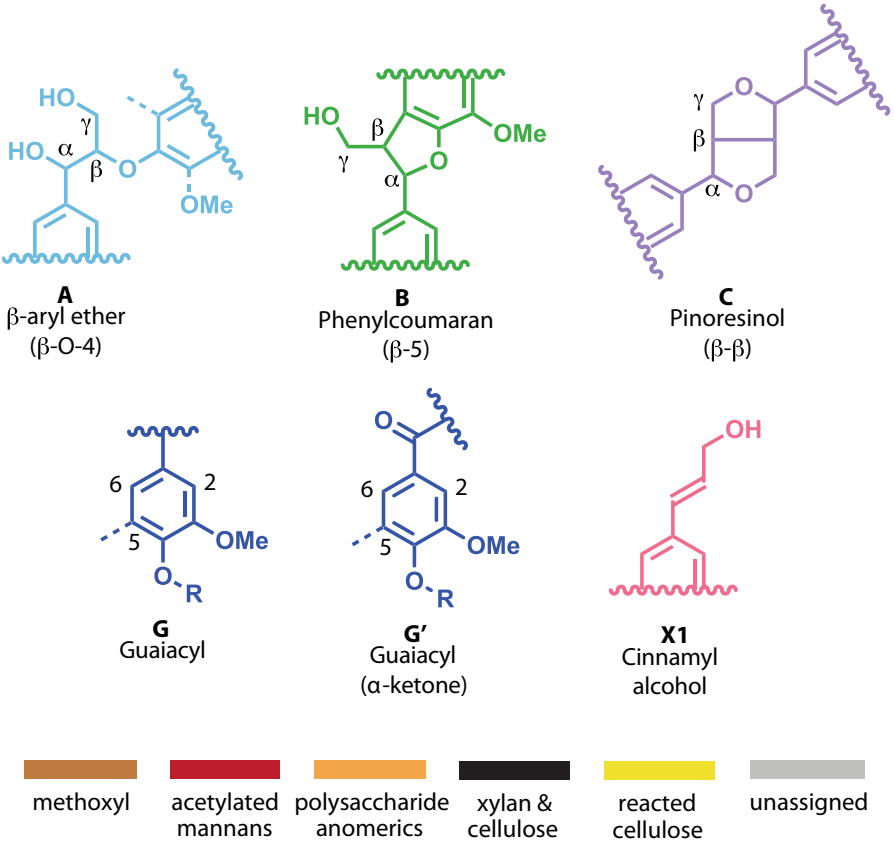

Fig. 3 Key to the macromolecular structures found in the spectra in Figs. 4, 5, 6 and 7. The structures are: (A) *β*-aryl ether (*β*-O-4) in cyan, (B) phenylcoumaran (*β*−5) in green, (C) pinoresinol (*β*-*β*) in lavender, (X1) cinnamyl alcohol endgroups in pink, (G) guaiacyl in dark blue, and (G′) α-ketone version of guaiacyl in dark blue. The lignin methoxyl group is represented by–OMe in brown. The polysaccharide structures include: H-2/C-2 & H-3/C-3 correlations for the acetylated structure of *β*-D-Man*p* (2-*O*-Ac-*β*-D-Man*p*, 3-*O*-Ac-*β*-D-Man*p*, & 2,3-*O*-Ac-*β*-D-Man*p*) in dark red, and the anomeric H-1/C-1 correlations for the major polysaccharides—*β*-D-Glc*p*^{I}, internal *β*-D-glucopyranosyl units (cellulose); *β*-D-Man*p*^{I}, internal *β*-D-mannopyranosyl units (mannan); *β*-D-Xyl*p*^{I}, internal *β*-D-xylopyranosyl units (xylan); *β*-D-Gal*p*^{T}, terminal *β*-D-galactopyranosyl units (galactan); *α*-L-Ara*f*, *α*-L-arabinofuranosyl units (arabinan); 4-*O*-methyl-*α*-D-glucuronic acid units, (MeGlcA); and the reducing endgroups *α*- & *β*-D-Glc*p*^{R}, *α*-D-Man*p*^{R}, *β*-D-Xyl*p*^{R}, *β*-D-Gal*p*^{R} (α_{red} & β_{red}) in orange. Other structures include xylan and cellulose internal structures in black, reacted cellulose in yellow, and structures currently not assigned or unresolved in gray

To realize the structural changes that occurred during model wood degradation and subsequent impregnation treatments with the three organosilicons, we qualitatively and semi-quantitatively compared the spectra in four groups. The first group was the untreated undegraded wood and model degraded wood; the second group was the undegraded wood and model degraded wood treated with A1; the third group was the undegraded wood and model degraded wood treated with A2; and the fourth

group was the undegraded wood and model degraded wood treated with S1. These four groups are shown in Figs. 4, 5, 6 and 7, respectively.

We then used contour peak integration to semi-quantify selected cell wall polymer structures and referenced these peaks to the lignin methoxyl peak. Figure 8 shows the results of these volume integral analyses.

From the spectra of the untreated model wood (Fig. 4) along with the integration data (Fig. 8), the lignin subunits *β*-O-4, *β*−5, *β*-*β*, and guaiacyl (G-2), showed that the CP and BP samples gave similar subunit frequencies. Only minor amounts of *β*-O-4 subunits were removed, and native acetyl groups on mannan were more heavily removed after biological degradation. In comparing the untreated CP to BP (Fig. 4), it is evident from the spectra in the anomeric region that arabinan, galactan, and much of the mannan were effectively removed. The ChP samples, compared to the CP samples, showed depletion of *β*−5 subunits, which led to minor losses in guaiacyl units. Depletion of mannan led to complete removal of the acetyl groups. Partial removal of galactan and glucan (cellulose) was also evident during chemical degradation (Yelle and Broda 2025).

When the model wood was treated with methyltrimethoxysilane (A1), the spectra (Fig. 5) showed quite similar spectral characteristics to all model woods (Fig. 4). For example, the *β*-O-4, *β*−5, guaiacyl (G-2), acetyl groups, as well as *α*- and *β*-reducing endgroups of polysaccharides were not altered dramatically. However, with all of the model woods (i.e., CP-A1, BP-A1, and ChP-A1), we observed that the *β*−5 subunits and guaiacyl lignin (G-2) were increased after A1 treatment, a circumstance demonstrating that demethoxylation must be occurring to a minor degree as was observed in other studies on wood treated with alkoxysilanes (Hill et al. 2007; van Opdenbosch et al. 2013). The oxidized guaiacyl units were evidenced by the elevated presence of the *α*-carbonyl (G-2′), which was slightly higher in biologically degraded wood.

When the model wood was treated with (3-mercaptopropyl)trimethoxysilane (A2), the spectra (Fig. 6) showed more dramatic differences as compared to both of the untreated model woods (Fig. 4). For example, the *α*-carbonyl (G-2′) was much higher than in all other treatment types, showing depolymerization of lignin. Furthermore, the polysaccharides were heavily cleaved, as evidenced by the tremendous increase in *α*- and *β*-reducing endgroups. With the chemically degraded pine (ChP-A2), we observed that the *β*-O-4 and guaiacyl lignin were more steadfast as compared to the untreated pine (CP-A2), suggesting that the alkali degraded pine is more resistant to further lignin depolymerization by A2 treatment as compared to the untreated contemporary pine. Overall, the A2 treatment seems to further depolymerize cell wall polymers beyond the already partial degradation that occurred via the model wood preparation

When the model wood was treated with the 1,3-Bis-[(diethylamino)−3-(propoxy) propan-2-ol]−1,1,3,3-tetramethyldisiloxane (S1), much different chemistry was observed (Fig. 7). In this case, we observed reduction of α-carbonyls (G-2′); the G-2′ contour peaks were almost absent in the CP-S1 spectrum and completely absent in the BP-S1 and ChP-S1 spectra. Moreover, like that of alkoxysilanes, we observed demethoxylation of the guaiacyl units; guaiacyl lignin (G-2) was slightly higher in the chemically treated model wood as compared to the untreated model wood.

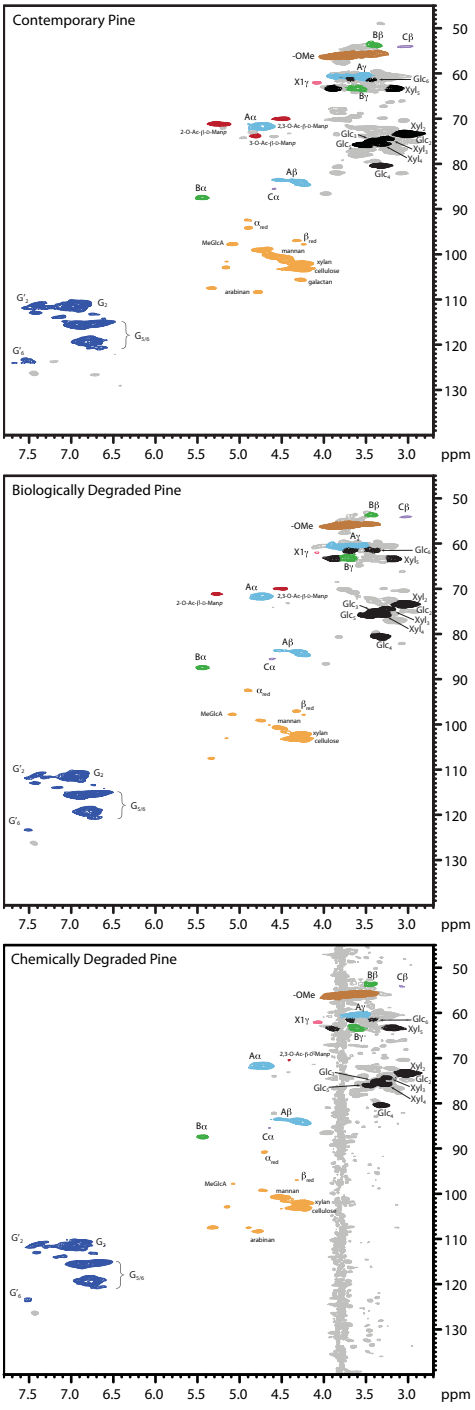

Fig. 4 Partial HSQC NMR spectra of untreated model degraded pine wood showing contemporary pine, biologically degraded pine, and chemically degraded pine, respectively. The selected contour colors and labels can be matched to their respective structure in Fig. 3

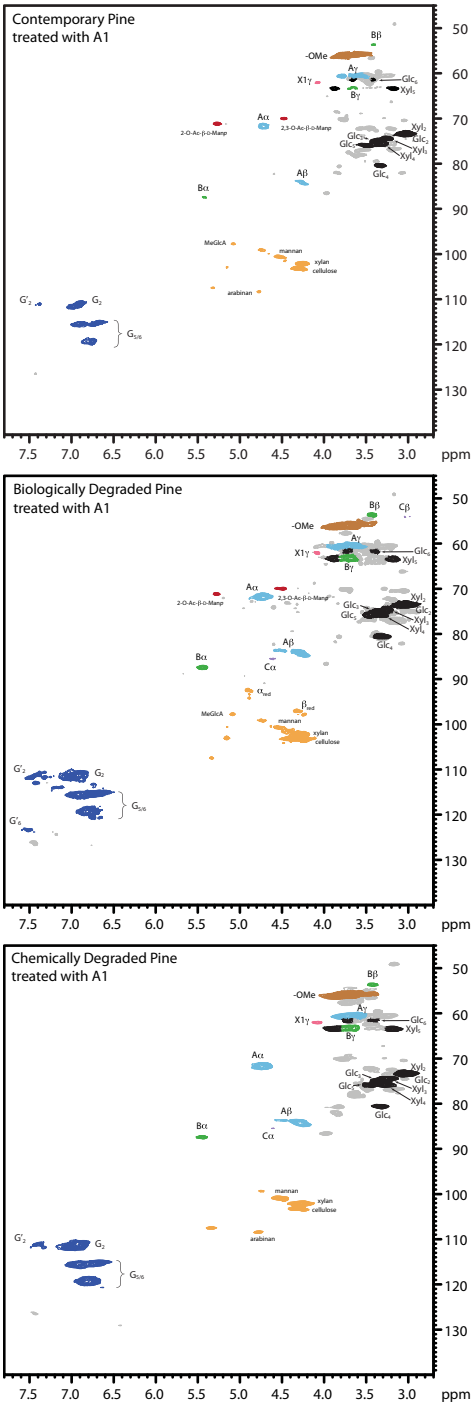

Fig. 5 Partial HSQC NMR spectra of model degraded pine wood treated with A1 showing contemporary pine, biologically degraded pine, and chemically degraded pine, respectively. The selected contour colors and labels can be matched to their respective structure in Fig. 3

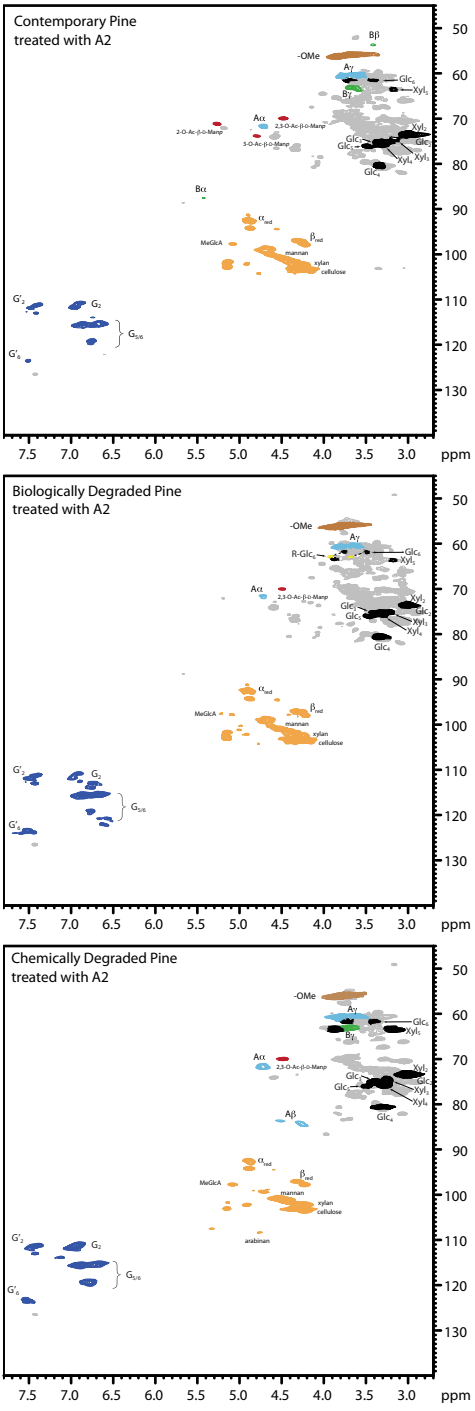

Fig. 6 Partial HSQC NMR spectra of model degraded pine wood treated with A2 showing contemporary pine, biologically degraded pine, and chemically degraded pine, respectively. Note: in the biologically degraded pine spectra, R-Glc$_6$ represents tentatively assigned contours from reactivity between treatment A2 and cellulose C$_6$ hydroxyls. The selected contour colors and labels can be matched to their respective structure in Fig. 3

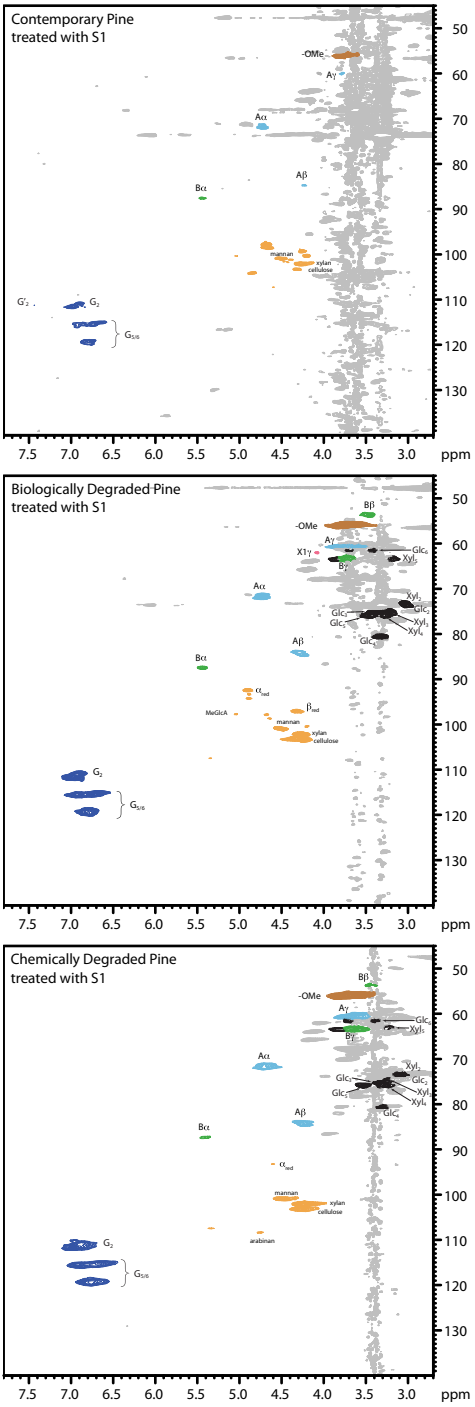

Fig. 7 Partial HSQC NMR spectra of model degraded pine wood treated with S1 showing contemporary pine, biologically degraded pine, and chemically degraded pine, respectively. The selected contour colors and labels can be matched to their respective structure in Fig. 3

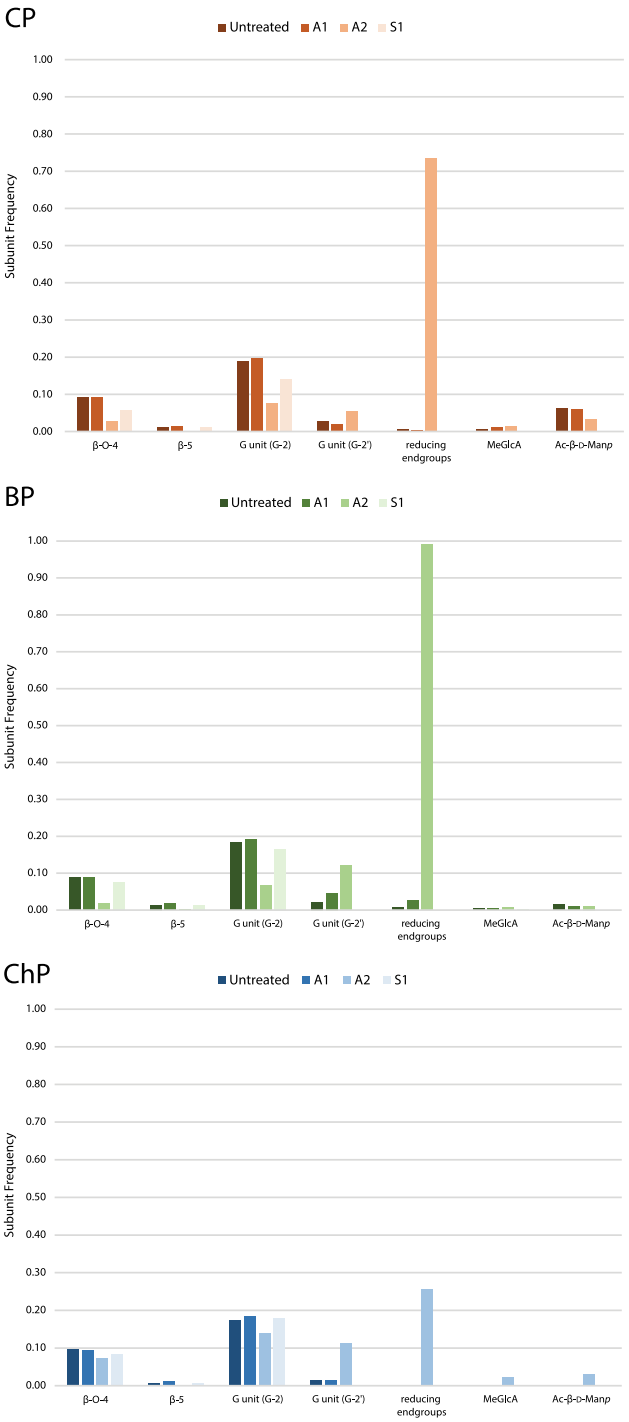

Fig. 8 Integration of selected cell wall polymer subunit peaks showing their frequency relative to the lignin methoxyl group. Sound contemporary pine (CP) is shown with reddish shaded bars, biologically degraded pine (BP) is shown with green shaded bars, and chemically degraded pine (ChP) is shown with blue shaded bars. Each bar graph displays a legend that is color-coded to the corresponding impregnation treatment (Untreated, A1, A2, or S1)

Table 1 Selected properties of sound control pine (CP), biologically degraded pine (BP), and chemically degraded pine (ChP) wood; EMC – maximum measured equilibrium moisture content (Broda et al. 2022a, b)

Wood property	CP	BP	ChP
Mass loss (%)	-	38.5 ± 4.7	16.8 ± 1.4
Bulk density (g cm^{-3})	0.44 ± 0.02	0.44 ± 0.03	0.65 ± 0.02
Total pore volume (cm^3 g^{-1})	0.0007	0.0015	0.0012
Free hydroxyls (mmol g^{-1})	7.9 ± 0.1	8.0 ± 1	1.3 ± 0.3

Table 2 Effectiveness of organosilicon treatment of sound control pine (CP), biologically degraded pine (BP), and chemically degraded pine (ChP) wood expressed as *WPG* – weight% gain, S_v – volumetric shrinkage, and ASE_v – volumetric anti-shrink efficiency (Broda et al. 2024)

Wood ID	WPG (%)	S_v (%)	ASE_v (%)
CP			
Untreated	-	-	-
A1	26.2 ± 5.1	−0.2 ± 0.2	-
A2	32.7 ± 5.6	−2.1 ± 0.7	-
S1	31.2 ± 5.7	−0.7 ± 0.3	-
BP			
Untreated	-	22.3 ± 0.9	-
A1	53.6 ± 7.6	4.6 ± 0.2	79.4
A2	63.3 ± 4.2	4.0 ± 1.3	82.1
S1	64.0 ± 3.2	5.5 ± 0.3	75.3
ChP			
Untreated	-	25.5 ± 3.8	-
A1	41.5 ± 5.6	12.3 ± 1.7	51.7
A2	53.2 ± 4.8	6.5 ± 1.6	74.5
S1	51.5 ± 4.7	6.6 ± 2.4	74.1

Another intriguing observation in the case of S1 was the complete removal of the α- and β-reducing endgroups.

Discussion

One of the main objectives of this study is to understand how each organosilicon treatment affects wood cell wall stabilization at the polymer structure level and if the new information obtained can explain the differences between the selected properties of analyzed wood types observed in our previous research. To assist in this, several structural and physical properties of the CP, BP, and ChP wood were measured previously and are presented in Tables 1 and 2. The following is a discussion of how the NMR data may explain some of these observations.

Sound contemporary pine (CP)

Methyltrimethoxysilane (A1)

When comparing the relative integrals of the lignin subunits in untreated CP to those in the A1-treated CP (Fig. 8), we observed minor changes to lignin and polysaccharides. However, from the spectra (Fig. 5), the A1 treatment did indeed lead to a depletion in cell wall polymers as all contours are at lower intensity compared to

the untreated CP. The depletion did not seem to show a preference for one cell wall polymer over the other. Instead, the A1 treatment depolymerized cell wall polymers rather equally throughout the sample.

The G-2 frequency in A1-treated CP (Fig. 8) showed a slight increase (~5%). Since all volume integrals are referenced to the lignin methoxyl group, the only way to have an increase in aromatics is by methoxyls decreasing. Therefore, demethoxylation must occur to some extent with the A1 treatment.

The effectiveness of the A1 treatment on CP (Table 2) showed a weight-percent gain (*WPG*) of 26.2% and a volumetric shrinkage (S_v) of −0.2%, indicating that with the comparatively low *WPG*, the treatment infiltrated and modified the polymers uniformly, allowing for effective dimensional stability. Part of A1's effectiveness may be attributed to its lower molecular weight and less bulkiness of the chemical compounds compared to the A2 and S1 treatments, making A1 more effectively infiltrate wood tissue with the relatively smaller total pore volume (0.0007 $cm^3\ g^{-1}$) in undegraded CP cell walls (Broda et al. 2024), and to position itself for reactions with cell wall polymers.

(3-Mercaptopropyl)trimethoxysilane (A2)

Some major differences between the untreated CP and the A2-treated CP were observed, especially within the lignin polymer. For example, the *β*-O-4 and *β*−5 subunit linkages decreased by greater than 60% (Fig. 8), while *β*-*β* subunits were completely removed (Fig. 6). The removal of these linkages suggests that the lignin polymer has been truncated by the A2 treatment; the native lignin polymer remains intact, but much of the lignin has been cleaved. It is not clear from these data if the silane reacted with lignin; typically, when a lignin hydroxyl group is reacted, a new chemical shift will appear downfield from the original hydroxyl group chemical shift, but this was not observed in the spectra (Fig. 6). Evidence of guaiacyl unit alteration was also confirmed via the aromatic region with approximately 60% depletion in native guaiacyl units (G-2), with a 50% increase in *α*-carbonyls (G-2′).

The treatment was equally harsh on the polysaccharides with *α*- and *β*-reducing endgroups highly elevated and removal of arabinan and galactan. The acetyl groups on mannan in A2-treated CP showed a decrease compared to the untreated CP, evidence of acetic acid releasing during treatment.

The effectiveness of the A2 treatment on CP (Table 2) showed a *WPG* of 32.7% and a S_v of −2.1%, suggesting that the treatment led to a slight swelling of the cell walls. Overall, the A2 treatment on CP was effective at maintaining dimensional stability. Compared to treatment A1, the A2 treatment gave slightly higher *WPG*, which may be attributed to its higher molecular weight. Even so, A2 was still effective at infiltrating the cell wall pores and able to react with available cell wall hydroxyls (Broda et al. 2024).

1,3-Bis-[(diethylamino)−3-(propoxy)propan-2-ol]−1,1,3,3-tetramethyldisiloxane (S1)

The siloxane, S1, treatment behaved somewhat differently than the alkoxylsilanes, A1 and A2. The *β*-O-4 subunits decreased by 37% while the *β*−5 subunits decreased by 15%; *β*-*β* subunits were completely removed (Fig. 7). The lignin guaiacyl units also decreased by 24%, with the complete removal of the G-2′ and G-6′, suggesting that reduction may be occurring. Polysaccharides were also heavily degraded, but *α*- and *β*-reducing ends were missing along with the 4-*O*-methyl-*α*-D-glucuronic acid units, indicating that carboxylic acid reduction chemistry must be at play here (Fig. 7).

Reduction chemistry by siloxanes, including tetramethyldisiloxane in the reduction of α,β-unsaturated carbonyl derivatives, has been reported in the literature (Larson and Fry 2008; Pesti and Larson 2016; Broda and Yelle 2022). To test whether the NMR solvent (DMSO-d_6) could be involved in facilitating the reduction of the *α*-carbonyls on guaiacyl units, we dissolved the same contemporary pine samples—treated with A1, A2, and S1—in dimethylacetamide-d_9. Dimethylacetamide-d_9 is an alternative wood cell wall dissolution solvent that swells the cell wall polymers and effectively dissolves lignin. The HSQC NMR spectra, focusing on the aromatic region, are shown in supplementary information, Figure S.I. 1. From these supporting spectra, we were able to confirm that the reduction was not brought about from the dissolution solvent since the *α*-carbonyls, depicted by the G-2′ and G-6′ peaks, were absent just as was observed in the CP sample treated with S1. More research is needed to further investigate the mechanisms involved in the reductive properties of siloxanes in wood cell walls.

We also observed a major depletion of the native cellulose, as indicated by the low-intensity anomeric peak at 4.25/103.7 ppm (Fig. 7). Cellulose was still strong in all of the alkoxysilane-treated wood samples, so this indicates that the siloxane treatments are able to heavily modify cellulose in CP, an observation also found before (Broda and Yelle 2022). The acetylated mannan signals, were, in this case, completely removed (Fig. 7).

The *WPG* for the S1 treatment of CP was 31.2%, which was similar to the A2 treatment. S_v was −0.7%, showing that even though the S1 molecule is large and bulky, it was effective at keeping the wood dimensions stable. In previous research, we determined that S1 can infiltrate the cell wall and also fill cell lumina, thus contributing to wood dimensional stabilization (Broda et al. 2024). It is likely that the cellulose degradation and effective reactivity with hydroxyls from cellulolytic degradation products, in particular, keep water from infiltrating the cell walls, further enhancing wood dimensional stability.

Biologically degraded pine (BP)

As the mass loss of the BP samples was 39%, this mass loss was attributed to the removal of arabinan, galactan, and much of the mannan since the lignin was not removed. As the organism utilized in this study was *Coniophora puteana* (a brown rot fungus), it has a preference for depolymerizing and metabolizing polysaccha-

rides—including hemicelluloses and cellulose—as well as deacetylating mannan (Schmidt 2006; Beck et al. 2018); however, part of lignin is also degraded or modified to some extent (Yelle et al. 2008b, 2011b; Martínez et al. 2011; Rese et al. 2025). Having a two-fold increase in total pore volume (0.0015 $cm^3\ g^{-1}$) over that of CP (0.0007 $cm^3\ g^{-1}$) should allow for higher *WPG*s, improved treatment infiltration, and potentially higher reactivity with cell wall polymers.

Methyltrimethoxysilane (A1)

As was found with the A1 treatment in CP, the BP did not experience dramatic changes to cell wall polymers; lignin subunit linkages and polysaccharides remained mostly unaltered (Fig. 5). The α-carbonyls (G-2′) did increase, indicating that oxidation of the aromatic units occurred, along with increased α- and β-reducing ends (Fig. 8).

The β−5 and G-2 frequencies in A1-treated BP (Fig. 8) also showed slight increases. Therefore, demethoxylation must be occurring to some extent with the A1 treatment in BP as well.

Overall, the A1 treatment of BP was effective at infiltrating the cell wall, with a *WPG* of 53.6% and lowering the S_v from 22.3 to 4.6% (Broda et al. 2024). With the slightly higher free hydroxyl content, 8.0 mmol g^{-1}, over the CP wood (7.9 mmol g^{-1}) and the removal of arabinan, galactan, much of the mannan, and demethylation by brown rot fungi, it is possible that the A1 treatment is more reactive towards the now more exposed lignin hydroxyls in the BP wood.

(3-Mercaptopropyl)trimethoxysilane (A2)

Depolymerization of the lignin and polysaccharides by the A2 treatment was evident in the BP, similar to that of the CP. However, the depolymerization of β-O-4 and β−5 subunit linkages was even more dramatic in the BP, with losses of 78% and 93%, respectively (Fig. 8), with complete removal of β-β subunits (Fig. 6). Like the A2 treatment in CP, the removal of these linkages suggests that the lignin polymer has similarly been truncated by the A2 treatment. It is not clear from these data if the silane reacted with the truncated lignin, as new downfield shifts were not observed. Heavy oxidation to lignin aromatics (G-2) was evident with an elevated G-2′.

Polysaccharide depolymerization was evident with a dramatic increase in α- and β-reducing endgroups in polysaccharides. Reactivity with cellulose C6-hydroxyls was evidenced by new peaks at 3.73/63.05 ppm and 3.93/63.05 ppm (Fig. 6). This cellulose reactivity at C6 was also observed when archeological elm wood was treated with (3-mercaptopropyl)trimethoxysilane (Broda and Yelle 2022). Almost all of the acetyl groups on the mannan were removed; the 2,3-*O*-Ac-β-D-Man*p* remained steadfast.

The A2 treatment of BP was effective at cell wall infiltration, with a *WPG* of 63.3% and lowering the S_v from 22.3 to 4.0% (Broda et al. 2024). The higher *WPG* with A2 compared to the A1 treatment in BP wood (a difference of almost 10%), along with the removal of arabinan, galactan, much of the mannan, and demethylation by brown rot fungi, likely led to a higher reactivity between A2 and the more exposed lignin and cellulose in the BP wood.

1,3-Bis-[(diethylamino)−3-(propoxy)propan-2-ol]−1,1,3,3-tetramethyldisiloxane (S1)

With the siloxane S1 treatment on BP, we observed less alteration of lignin subunits and polysaccharides as compared to CP. For example, the *β*-O-4 subunits decreased by 13% while the *β*−5 subunits remained the same (Fig. 8); *β*-*β* subunits were removed entirely (Fig. 7). Reduction of guaiacyl *α*-carbonyls was observed once again in BP by the absence of G-2′ and G-6′ peaks.

We did not observe a major depletion of native cellulose, as indicated by the steadfast anomeric peak at 4.25/103.7 ppm (Fig. 7). Therefore, cellulose depolymerization was not a factor here, as was seen in other cases of siloxane treatments on wood. We did see complete removal of the acetyl groups on mannan, as well as a disappearance of reducing endgroups and 4-*O*-methyl-*α*-D-glucuronic acid units as was similarly observed in the CP sample treated with S1.

The lessened depolymerization in cell wall polymers, lignin, and cellulose with the S1 treatment on BP suggests that the remaining lignin subunits and polysaccharides after brown rot decay were either less accessible or less reactive with the S1 treatment.

Even though S1 can both infiltrate the cell walls and fill cell lumina, leading to a *WPG* of 64.0%, the S1 treatment was not as effective as the A1 and A2 treatments on BP as shown by the higher S_v of 5.5% and lower ASE_v of 75%.

Chemically degraded pine (ChP)

From Table 1, the mass loss of the ChP was 17%, much lower than that of the BP. Most of the mass loss was attributed to some lignin subunit removal along with major depletions in polysaccharides (e.g., mannan, galactan, and glucan), as well as deacetylation of mannan when compared to CP. The overall bulk density increased from 0.44 g cm^{-1} to 0.65 g cm^{-1} after ChP preparation and air-drying, suggesting infiltration of organosilicons may be more challenging. However, the total pore volume of 0.0012 cm^3 g^{-1} may compensate for the higher density and facilitate accessibility. The free hydroxyl content decreased from 7.9 mmol g^{-1} in CP to 1.3 mmol g^{-1} in ChP, which may lead to lower reactivity of organosilicons with wood polymers.

Methyltrimethoxysilane (A1)

The A1 treatment of ChP resulted in only minor alterations of the existing cell wall polymers. The changes observed were increased *β*−5 subunits and guaiacyl unit (G-2) frequencies. Similar to what we observed in the A1-treated CP and BP, demethoxylation must be occurring to some extent with the A1 treatment in ChP as well (Fig. 8).

Other notable changes were the loss of acetyl groups on mannan, the 4-*O*-methyl-*α*-D-glucuronic acid and the *α*- and *β*-reducing endgroups (Figs. 5 and 8).

The *WPG* of the A1 treatment of ChP was 41.5% with a S_v of 12.3% and an ASE_v of 52%, compared to a S_v of 25.5% for untreated ChP. Therefore, the effectiveness of ChP wood treated with A1 was not as high as what we have seen with the CP and BP.

As free hydroxyls were shown to be low, this may be a major hindrance in A1 treatment reactivity with wood polymers.

(3-Mercaptopropyl)trimethoxysilane (A2)

As we observed in the A2 treatment of BP, depolymerization of lignin and polysaccharides was evident, with a 25% depletion in *β*-O-4 subunits and removal of *β*−5 and *β*-*β* subunit linkages along with cinnamyl alcohol endgroups (X1) (Figs. 6 and 8). Furthermore, the guaiacyl units (G-2) were depleted while the *α*-carbonyls (G-2′) were elevated, indicating a highly oxidized lignin.

These ligninolytic transformations by the A2 treatment suggest that a similar lignin depolymerization mechanism must be at work here for all model wood sample types. For example, thiols are known to mediate nucleophilic substitution reactions leading to ether cleavage (Klinger et al. 2020). Acidolysis cleaves the arylglycerol-*β*-aryl ether (*β*-O-4) bond, leading to Hibbert's ketones, one such structure being the α-ketone (Sarkanen and Ludwig 1971; Adler 1977; Imai et al. 2011). The proposed mechanism involves acid-catalyzed dehydration to an enol ether, followed by hydrolysis to cleave the *β*-O-4. Allylic rearrangement leads to ketone formation. With the significant release of acetyls from galactoglucomannans with the A2 treatment, acidolysis is hypothesized to occur.

The polysaccharides also showed evidence of depolymerization with *α*- and *β*-reducing endgroups elevated, along with a depletion of arabinan (Figs. 6 and 8).

The *WPG* of A2-treated ChP was 53.2% with a S_v of 6.5% and an ASE_v of 75%, which is a dramatic improvement over that of A1-treated ChP. It is likely that the further wood depolymerization afforded by the A2 treatment on ChP led to increased reactivity and effectively stabilizing its dimensions.

1,3-Bis-[(diethylamino)−3-(propoxy)propan-2-ol]−1,1,3,3-tetramethyldisiloxane (S1)

The S1 treatment on ChP, as was observed with the BP, did not dramatically alter cell wall polymers. The *β*-O-4 subunit linkages did decrease slightly, with the removal of the *β*-*β* subunit linkages, but *β*−5 subunit linkages remained unaltered. Similar to the A2 treatment, the cinnamyl alcohol endgroups (X1) were removed (Figs. 7 and 8).

Reduction of the *α*-carbonyl of guaiacyl units (G-2′) was observed in the S1-treated CP, BP, and ChP spectra (Fig. 7), confirming that reduction of *α*-carbonyls is a common phenomenon with these siloxanes. Demethoxylation of the guaiacyl units, as determined by the slight elevation in frequency of guaiacyl lignin (G-2) in the chemically treated model wood as compared to the untreated model wood (Fig. 8), suggests that regardless of organosilicon used for impregnation, demethoxylation is likely to occur. These two reactions (*α*-ketone reduction and demethoxylation) were also observed in our previous study with archaeological elm wood (Broda and Yelle 2022). Literature also suggests that reduction of α,β-unsaturated carbonyl derivatives by siloxanes is a likely scenario here (Larson and Fry 2008; Pesti and Larson 2016).

Polysaccharide depolymerization was also evident from the spectra, with much of the α- and β-reducing endgroups removed, along with acetyl groups on mannan, 4-*O*-methyl-α-D-glucuronic acid units and arabinan (Figs. 7 and 8).

With a *WPG* of 51.5%, a S_v of 6.6%, and an ASE_v of 74%, the S1 treatment of ChP shared similar effectiveness to that of the A2 treatment, although with a much milder cell wall depolymerization, which suggests different stabilizing mechanisms of these two compounds. The low free hydroxyl content of ChP may be less of a factor here for effective stabilization. Further research is underway to better understand these unique siloxane reaction mechanisms occurring with wood cell wall polymers.

Conclusion

Conserving ancient wooden artifacts is critical in preserving history and retelling stories that would otherwise be lost. This research allows for understanding the mechanisms of treatments used to stabilize these fragile and historical wooden objects. Organosilicons are highly effective as wood stabilizers. Here, we have characterized model degraded wood and how various organosilicon impregnations affect the chemistry of the wood cell wall polymers. By using wood dissolution techniques and HSQC NMR we found that the alkoxysilane A1 was the mildest towards native wood polymer depolymerization, while the alkoxysilane with the mercaptopropyl group (A2) showed the most dramatic depolymerization of both the lignin and polysaccharides for all model woods, especially in the case of biologically treated wood. The siloxane (S1) impregnation led to some cell wall depolymerization in the model woods, but was not as much as seen with the A2 treatment; complete removal of α-carbonyls (G-2′ and G-6′) and α- and β-reducing endgroups in polysaccharides was evident in all the S1 samples.

This study revealed that the biologically degraded and chemically degraded model woods were effective in allowing the organosilicons to access the cell wall free volume, react with cell wall polymers, and stabilize cell wall dimensions. We hypothesize that, during organosilicon treatment, some wood cell wall depolymerization is necessary so that the silane or siloxane is able to infiltrate deeply into the cell wall matrices and, once reacted, is similar to a healing process where the truncated wood polymers are able to meld together.

Supplementary Information The online version contains supplementary material available at https://doi.org/10.1007/s00226-025-01673-3.

Author contributions This manuscript was written with contributions from all authors. All authors have approved the final version of the manuscript. D.J.Y. and M.B. conceptualized, planned and performed all experiments, D.J.Y. prepared all figures, D.J.Y. and M.B. wrote the main manuscript text.

Funding NMR studies were supported by the Polish-U.S. Fulbright Commission through a Fulbright Senior Award 2020/21 granted to Magdalena Broda and funded by USDA Forest Products Laboratory, Madison, Wisconsin, USA.

Data availability No datasets were generated or analysed during the current study.

Declarations

Competing interests The authors declare no competing interests.

References

Adler E (1977) Lignin chemistry—past, present and future. Wood Sci Technol 11(3):169–218
Afshar R, Cheylan M, Almkvist G et al (2020) Creep in oak material from the Vasa ship: verification of linear viscoelasticity and identification of stress thresholds. Eur J Wood Prod 78:1095–1103. https://doi.org/10.1007/s00107-020-01566-1
Albelda Berenguer M, Monachon M, Jacquet C et al (2019) Biological oxidation of sulfur compounds in artificially degraded wood. Int Biodeter Biodegr 141:62–70. https://doi.org/10.1016/j.ibiod.2018.06.009
Bakri MKB, Jayamani E, Hamdan S et al (2016) Fundamental study on the effect of alkaline treatment on natural fibers structures and behaviors. J Eng Appl Sci 11:8759–8763
Beck G, Hegnar OA, Fossdal CG, Alfredsen G (2018) Acetylation of Pinus radiata delays hydrolytic depolymerisation by the brown-rot fungus rhondonia placenta. Int Biodeterior Biodegrad 135:39–52. https://doi.org/10.1016/j.ibiod.2018.09.003
Belt T, Altgen M, Awais M et al (2024) Degradation by brown rot fungi increases the hygroscopicity of heat-treated wood. Int Biodeterior Biodegrad 186:105690. https://doi.org/10.1016/j.ibiod.2023.105690
Björdal CG, Daniel G, Nilsson T (2000) Depth of burial, an important factor in controlling bacterial decay of waterlogged archaeological Poles. Int Biodeterior Biodegrad 45:15–26. https://doi.org/10.1016/S0964-8305(00)00035-4
Blanchette RA, Nilsson T, Daniel G, Abad A (1989) Biological degradation of wood. Archaeological wood. American Chemical Society, pp 141–174
Broda M, Hill CA (2021) Conservation of waterlogged Wood—Past, present and future perspectives. Forests 12:1193. https://doi.org/10.3390/f12091193
Broda M, Plaza NZ (2023) Durability of model degraded wood treated with organosilicon compounds against fungal decay. Int Biodeter Biodegr 178:105562. https://doi.org/10.1016/j.ibiod.2022.105562
Broda M, Yelle DJ (2022) Reactivity of waterlogged archeological elm wood with organosilicon compounds applied as wood consolidants: 2D 1H–13 C Solution-State NMR studies. Molecules 27:3407. https://doi.org/10.3390/molecules27113407
Broda M, Dąbek I, Dutkiewicz A et al (2020) Organosilicons of different molecular size and chemical structure as consolidants for waterlogged archaeological wood–a new reversible and retreatable method. Sci Rep 10:1–13. https://doi.org/10.1038/s41598-020-59240-8
Broda M, Popescu C-M, Curling SF et al (2022a) Effects of biological and chemical degradation on the properties of Scots pine Wood—Part I: chemical composition and microstructure of the cell wall. Materials 15:2348. https://doi.org/10.3390/ma15072348
Broda M, Spear MJ, Curling SF, Dimitriou A (2022b) Effects of biological and chemical degradation on the properties of Scots Pine—Part II: Wood-Moisture relations and viscoelastic behaviour. Forests 13:1390. https://doi.org/10.3390/f13091390
Broda M, Jakes JE, Li L, Antipova OA (2023) Archeological wood conservation with selected organosilicon compounds studied by XFM and nanoindentation. Wood Sci Technol 57:1277–1298. https://doi.org/10.1007/s00226-023-01503-4
Broda M, Jakes JE, Li L et al (2024) Conservation of model degraded pine wood with selected organosilicons studied by XFM and nanoindentation. Wood Sci Technol 58:649–675. https://doi.org/10.1007/s00226-024-01533-6
Broda M, Plaza NZ, Jakes JE et al (2025) Effect of alkali treatment and fungal degradation on the nanostructure and cellulose arrangement in Scots pine cell walls– A neutron and X-ray scattering study. Carbohydr Polym 347:122733. https://doi.org/10.1016/j.carbpol.2024.122733
de Graaf RA, Nicolay K (1997) Adiabatic rf pulses: applications to in vivo NMR. Concepts Magn Reson Educ J 9(4):247–268
Fliri L, Heise K, Koso T et al (2023) Solution-state nuclear magnetic resonance spectroscopy of crystalline cellulosic materials using a direct dissolution ionic liquid electrolyte. Nat Protoc 18:2084–2123. https://doi.org/10.1038/s41596-023-00832-9

Franceschi E, Cascone I, Nole D (2008) Study of artificially degraded woods simulating natural ageing of archaeological findings. J Therm Anal Calorim 92:319–322. https://doi.org/10.1007/s10973-007-8722-3

Gérardin P (2016) New alternatives for wood preservation based on thermal and chemical modification of wood— a review. Ann for Sci 73:559–570. https://doi.org/10.1007/s13595-015-0531-4

Glastrup J, Shashoua Y, Egsgaard H, Mortensen MN (2006) Degradation of PEG in the warship Vasa. Macromolecular Symposia 238:22–29. https://doi.org/10.1002/masy.200650604

Grattan DW (1987) 3 - Waterlogged wood. In: Pearson C (ed) Conservation of marine archaeological objects. Butterworth-Heinemann, Oxford, pp 55–67

Grattan D, Bilz M, Grant T, Logan J (2006) Outcome determines treatment – An approach to the treatment of waterlogged wood. J Wetl Archaeol 6:49–63. https://doi.org/10.1179/jwa.2006.6.1.49

Han L, Guo J, Tian X et al (2022) Evaluation of PEG and sugars consolidated fragile waterlogged archaeological wood using nanoindentation and ATR-FTIR imaging. Int Biodeterior Biodegrad 170:105390. https://doi.org/10.1016/j.ibiod.2022.105390

Han L, Han X, Liang G et al (2023) Even samples from the same waterlogged wood are hygroscopically and chemically different by simultaneous DVS and 2D COS-IR spectroscopy. Forests 14:15. https://doi.org/10.3390/f14010015

Hedenström M, Wiklund-Lindström S, Öman T et al (2009) Identification of lignin and polysaccharide modifications in Populus wood by chemometric analysis of 2D NMR spectra from dissolved cell walls. Mol Plant 2:933–942. https://doi.org/10.1093/mp/ssp047

Hill CAS (2007) Wood modification: chemical, thermal and other processes. Wiley

Hill CA, Farahani MM, Hale MD (2004) The use of organo alkoxysilane coupling agents for wood preservation. https://doi.org/10.1515/HF.2004.049

Hoffmann P (2010) On the long-term visco-elastic behaviour of polyethylene glycol (PEG) impregnated archaeological oak wood. Holzforschung 64:725–728. https://doi.org/10.1515/hf.2010.082

Hoffmann P, Jones MA (1989) Structure and degradation process for waterlogged archaeological wood. Archaeological wood. American Chemical Society, pp 35–65

Holtman KM, Chang H, Kadla JF (2004) Solution-State nuclear magnetic resonance study of the similarities between milled wood lignin and cellulolytic enzyme lignin. J Agric Food Chem 52:720–726. https://doi.org/10.1021/jf035084k

Hossain MA, Rahaman MS, Yelle D et al (2021) Effects of polyol-based deep eutectic solvents on the efficiency of rice straw enzymatic hydrolysis. Ind Crops Prod 167:113480. https://doi.org/10.1016/j.indcrop.2021.113480

Ikeda T, Holtman K, Kadla JF, Chang HM, Jameel H (2002) Studies on the effect of ball milling on lignin structure using a modified DFRC method. J Agric Food Chem 50:129–135

Imai T, Yokoyama T, Matsumoto Y (2011) Revisiting the mechanism of β-O-4 bond cleavage during acidolysis of lignin IV: dependence of acidolysis reaction on the type of acid. J Wood Sci 57:219–225

Kavvouras PK, Kostarelou C, Zisi A et al (2009) Use of Silanol-Terminated polydimethylsiloxane in the conservation of waterlogged archaeological wood. Stud Conserv 54:65–76. https://doi.org/10.1179/sic.2009.54.2.65

Kennedy A, Pennington ER (2014) Conservation of chemically degraded waterlogged wood with sugars. Stud Conserv 59:194–201. https://doi.org/10.1179/2047058413Y.0000000109

Kim H, Ralph J (2010) Solution-state 2D NMR of ball-milled plant cell wall gels in DMSO-d6/pyridine-d5. Org Biomol Chem 8:576–591

King AWT, Mäkelä V, Kedzior SA et al (2018) Liquid-State NMR analysis of nanocelluloses. Biomacromolecules 19:2708–2720. https://doi.org/10.1021/acs.biomac.8b00295

Klinger GE, Zhou Y, Foote JA, Wester AM, Cui Y, Alherech M, Stahl SS, Jackson JE, Hegg EL (2020) Nucleophilic thiols reductively cleave ether linkages in lignin model polymers and lignin. ChemSusChem 13(17):4394–4399

Koso T, Rico del Cerro D, Heikkinen S et al (2020) 2D assignment and quantitative analysis of cellulose and oxidized celluloses using solution-state NMR spectroscopy. Cellulose 27:7929–7953. https://doi.org/10.1007/s10570-020-03317-0

Kupče E, Freeman R (2007) Compensated adiabatic inversion pulses: broadband INEPT and HSQC. J Magn Reson 187:258–265

Larson L, Fry GL (2008) Ionic and organometallic-catalyzed organosilane reductions. In: Denmark SE (ed) Organic reactions, 1st edn. Wiley, pp 1–737

Liu L, Zhang L, Zhang B, Hu Y (2019) A comparative study of reinforcement materials for waterlogged wood relics in laboratory. J Cult Herit 36:94–102. https://doi.org/10.1016/j.culher.2018.08.002

Lourenço A, Araújo S, Gominho J et al (2020) Structural changes in lignin of thermally treated eucalyptus wood. J Wood Chem Technol 40:258–268. https://doi.org/10.1080/02773813.2020.1769674
Lu F, Ralph J (2003) Non-degradative dissolution and acetylation of ball-milled plant cell walls: high-resolution solution-state NMR. Plant J 35:535–544. https://doi.org/10.1046/j.1365-313X.2003.01817.x
Lundquist K, Lundgren R (1972) Acid degradation of lignin, Part VII. The cleavage of ether bonds. Acta Chem Scand 26(5):2005–2023
Marais BN, Brischke C, Militz H (2022) Wood durability in terrestrial and aquatic environments – A review of biotic and abiotic influence factors. Wood Mater Sci Eng 17:82–105. https://doi.org/10.1080/17480272.2020.1779810
Martínez AT, Rencoret J, Nieto L et al (2011) Selective lignin and polysaccharide removal in natural fungal decay of wood as evidenced by in situ structural analyses. Environ Microbiol 13:96–107. https://doi.org/10.1111/j.1462-2920.2010.02312.x
Maunu SL (2002) NMR studies of wood and wood products. Progress Nucl Magn Reson Spectrosc 40:151–174. https://doi.org/10.1016/S0079-6565(01)00041-3
Miura K, Nakano T (2015) Analysis of mercerization process based on the intensity change of deconvoluted resonances of 13 C CP/MAS NMR: cellulose mercerized under cooling and non-cooling conditions. Mater Sci Engineering: C 53:189–195. https://doi.org/10.1016/j.msec.2015.04.006
Morgós A, Imazu S, Ito K (2015) Sugar conservation of waterlogged archaeological finds in the last 30 years. In: Proceedings of CONDITION. 2015 Conservation and Digitalization Conference, 19th–22nd May. pp 15–20
Mortensen MN, Egsgaard H, Hvilsted S et al (2012) Tetraethylene glycol thermooxidation and the influence of certain compounds relevant to conserved archaeological wood. J Archaeol Sci 39:3341–3348. https://doi.org/10.1016/j.jas.2012.05.032
Namyslo JC, Drafz MHH, Kaufmann DE (2021) Durable modification of wood by Benzoylation—Proof of covalent bonding by solution state NMR and DOSY NMR Quick-Test. Polymers 13:2164. https://doi.org/10.3390/polym13132164
Nishiyama Y, Kuga S, Okano T (2000) Mechanism of mercerization revealed by X-ray diffraction. J Wood Sci 46:452–457. https://doi.org/10.1007/BF00765803
Pandey KK, Pitman AJ (2003) FTIR studies of the changes in wood chemistry following decay by brown-rot and white-rot fungi. Int Biodeter Biodegr 52:151–160. https://doi.org/10.1016/S0964-8305(03)00052-0
Pesti J, Larson GL (2016) Tetramethyldisiloxane: a practical organosilane reducing agent. Org Process Res Dev 20:1164–1181. https://doi.org/10.1021/acs.oprd.6b00124
Reinprecht L (2016) Abiotic degradation of wood. Wood deterioration, protection and maintenance. Wiley, Ltd, pp 28–61
Rese M, van Erven G, Veersma RJ et al (2025) Detailed characterization of the conversion of hardwood and softwood lignin by a Brown-Rot basidiomycete. Biomacromolecules 26:1063–1074. https://doi.org/10.1021/acs.biomac.4c01403
Sandberg D, Kutnar A, Mantanis G (2017) Wood modification technologies - a review. Iforest 10:895. https://doi.org/10.3832/ifor2380-010
Sarkanen K, Ludwig C (1971) Lignins: occurrence, formation, structure and reactions. Wiley, New York, pp 354–359
Schmidt O (2006) Wood cell wall degradation. Wood and tree fungi: biology, damage, protection, and use. Springer, Berlin, pp 87–107
Smith CW (2002) A second set of experiments using hydrolyzable polymers to preserve waterlogged wood. Postprints of the wooden artifacts group. American Institute for Conservation of Historic and Artistic Works Wooden Artifacts Group
Spear MJ, Curling SF, Dimitriou A, Ormondroyd GA (2021) Review of functional treatments for modified wood. Coatings 11:327. https://doi.org/10.3390/coatings11030327
Tahira A, Howard W, Pennington ER, Kennedy A (2017) Mechanical strength studies on degraded waterlogged wood treated with sugars. Stud Conserv 62:223–228. https://doi.org/10.1080/00393630.2016.1169364
Unger A, Schniewind A, Unger W (2001) Conservation of wood artifacts: a handbook. Springer
van Opdenbosch D, Dörrstein J, Klaithong S et al (2013) Chemistry and water-repelling properties of phenyl-incorporating wood composites. Holzforschung 67:931–940. https://doi.org/10.1515/hf-2013-0011

Vorobyev A, van Dijk NP, Kristofer Gamstedt E (2019) Orthotropic creep in polyethylene glycol impregnated archaeological oak from the Vasa ship. Mech Time-Depend Mater 23:35–52. https://doi.org/10.1007/s11043-018-9382-3

Wakefield JMK, Braovac S, Kutzke H et al (2020) Tert-butyldimethylsilyl Chitosan synthesis and characterization by analytical ultracentrifugation, for archaeological wood conservation. Eur Biophys J 49:781–789. https://doi.org/10.1007/s00249-020-01450-z

Wu M, Han X, Qin Z et al (2022) A Quasi-Nondestructive evaluation method for Physical-Mechanical properties of fragile archaeological wood with TMA: A case study of an 800-Year-Old shipwreck. Forests 13:38. https://doi.org/10.3390/f13010038

Xu E, Wang D, Lin L (2020) Chemical structure and mechanical properties of wood cell walls treated with acid and alkali solution. Forests 11:87. https://doi.org/10.3390/f11010087

Yang G, An X, Yang S (2021) The effect of ball-milling time on the isolation of lignin in the cell wall of different biomass. Front Bioeng Biotechnol 9:807625

Yelle DJ, Broda M (2025) Characterizing the chemistry of artificially degraded Scots pine wood serving as a model of naturally degraded waterlogged wood using1H–13C HSQC NMR. Wood Sci Technol. https://doi.org/10.1007/s00226-024-01618-2

Yelle DJ, Ralph J (2016) Characterizing phenol–formaldehyde adhesive cure chemistry within the wood cell wall. Int J Adh Adh 70:26–36. https://doi.org/10.1016/j.ijadhadh.2016.05.002

Yelle DJ, Ralph J, Frihart CR (2008a) Characterization of nonderivatized plant cell walls using high-resolution solution-state NMR spectroscopy. MRC 46:508–517. https://doi.org/10.1002/mrc.2201

Yelle DJ, Ralph J, Lu F, Hammel KE (2008b) Evidence for cleavage of lignin by a brown rot basidiomycete. Environ Microbiol 10:1844–1849. https://doi.org/10.1111/j.1462-2920.2008.01605.x

Yelle DJ, Ralph J, Frihart CR (2011a) Delineating pMDI model reactions with loblolly pine via solution-state NMR spectroscopy. Part 2. Non-catalyzed reactions with the wood cell wall. Holzforschung 65:145–154. https://doi.org/10.1515/hf.2011.029

Yelle DJ, Wei D, Ralph J, Hammel KE (2011b) Multidimensional NMR analysis reveals truncated lignin structures in wood decayed by the brown rot basidiomycete postia placenta. Environ Microbiol 13:1091–1100. https://doi.org/10.1111/j.1462-2920.2010.02417.x

Yelle DJ, Kaparaju P, Hunt CG et al (2013) Two-Dimensional NMR evidence for cleavage of lignin and Xylan substituents in wheat straw through hydrothermal pretreatment and enzymatic hydrolysis. Bioenerg Res 6:211–221. https://doi.org/10.1007/s12155-012-9247-6

Yelle DJ, Kapich AN, Houtman CJ et al (2014) A highly diastereoselective oxidant contributes to lignin olysis by the white rot basidiomycete Ceriporiopsis subvermispora. Appl Environ Microbiol 80:7536–7544

Zelinka SL, Altgen M, Emmerich L et al (2022) Review of wood modification and wood functionalization technologies. Forests 13:1004. https://doi.org/10.3390/f13071004

Zhou Y, Zhang Z, Wu M et al (2024) Versatile cross-linking strategy using water-soluble silane and dialdehyde for consolidation and dehydration of waterlogged archaeological wood. Wood Sci Technol 59:20. https://doi.org/10.1007/s00226-024-01625-3

Zhu Y, Li W, Meng D et al (2022) Non-enzymatic modification of the crystalline structure and chemistry of Masson pine in brown-rot decay. Carbohydr Polym 286:119242. https://doi.org/10.1016/j.carbpol.2022.119242